Science and Justice 56 (2016) 329–340

Contents lists available at ScienceDirect

Science and Justice

journal homepage: www.elsevier.com/locate/scijus

Laser ablation coupled with DAPNe-NSI-MS applied to redacted documents

Vivian Huynh, Zachary J. Sasiene, Phillip M. Mach, Teresa D. Golden, Guido F. Verbeck *

Department of Chemistry, 1155 Union Circle #305070, University of North Texas, Denton, TX 76203, United States

ARTICLE INFO

Article history:
Received 8 October 2015
Received in revised form 15 January 2016
Accepted 2 June 2016

Keywords:
Nanospray mass spectrometry
Laser ablation
Document ink analysis
Nondestructive
Nanomanpulation
DAPNe

ABSTRACT

Laser ablation has been applied to redacted documents, where the text has been concealed by other ink. This technique strips the redacting ink revealing the text that was once redacted. Once removed, a nanomanipulation technique is used to extract the ink of the underlying text where mass spectrometry is then implemented to analyze its ink chemistry. In order to facilitate microscopy with direct analyte-probed nanoextraction coupled to nanospray ionization mass spectrometry (DAPNe-NSI-MS), laser ablation must be executed prior to ink extraction. Laser ablation has a nondestructive approach of stripping the ink used to redact the document. Not only does this reveal the text, it clears an area for DAPNe to directly extract ink, in miniscule amounts, from the document without inducing destruction. The redacting ink was concluded to affect the aging process of the concealed handwritten ink more than the printed text. The redacted handwritten sample obtained higher relative peak area (%) values than the control samples (text that was not redacted) and the control for the printed text produced higher amounts of low molecular weight products than the sample. Implementing laser ablation on these samples could also affect the chemical properties of the underlying ink due to the additional UV radiation and plasma heating. Results indicate by using laser ablation to remove the redacting ink, the relative peak area of the underlying ink deviates by 1.25%. The thermal degradation of binding agents such as polymethylene, polyethylene glycol, and diethylene glycol was monitored by calculating the relative peak area for five days which, in turn, tracks the oxidation process. The relative peak area values were also used to determine the chemical kinetics of polyethylene glycol, where degradation and polymerization occur.

© 2016 The Chartered Society of Forensic Sciences. Published by Elsevier Ireland Ltd. All rights reserved.

1. Introduction

Redacted documents have become a prominent issue when analyzing due to the concealed text. This method is normally done with a marker or pen that deposits ink over the document, which hides the information. The importance of analyzing redacted documents is to expose information that a subject attempted to hide. This could occur within the private sector, such as in the business division both for lawful and unlawful practices. Therefore, it is important to remove the ink used to conceal the written/printed text with the aim of revealing the passage and analyzing the ink underneath.

Ink analysis continues to play a significant role in questioned and authentic documents. The courts prefer nondestructive methods so most forensic approaches focus on nondestructive means of analysis, preventing undue alteration or introducing any aberrations. The most common nondestructive methods make use of visual microscopy [1] and video spectral comparisons (VSC) [1]. However, these methods can be defeated by the redaction process (i.e., specifically black-on-black or ink obliterations). With the help of a laser ablation (LA) method, visual microscopy and VSC can be used once the redacting ink is removed. The LA process is a nondestructive method which preserves the original text while providing a method to uncover the text that was once redacted. Other visual and chemical analyses can be performed due to the preservation of the remaining chemistry on the text [2]. Currently, research continues to investigate analysis of ink in combination with other nondestructive methods [2].

The use of diverse instruments to examine inks has been successful in identifying markers and unique characteristics of inks. Many manufacturers also include dopants into ink which make them easily identifiable; unfortunately these are proprietary to the company and are not made known to the public. Various methods utilizing separations and mass spectrometric techniques have yielded great results in analyzing different components of inks, dyes, and pigments [3–6]. Employing mass spectrometric procedures instead of chromatographic methods reduces sample preparation, time, and solvent needs. Separation techniques such as gas chromatography (GC) [7–9], high performance liquid chromatography (HPLC) [10–12], thin-layer chromatography (TLC) [13], and capillary electrophoresis [14] require destruction to the document when analyzing the ink. This includes removing a small portion of

* Corresponding author.
E-mail address: gverbeck@unt.edu (G.F. Verbeck).

http://dx.doi.org/10.1016/j.scijus.2016.06.002
1355-0306/© 2016 The Chartered Society of Forensic Sciences. Published by Elsevier Ireland Ltd. All rights reserved.

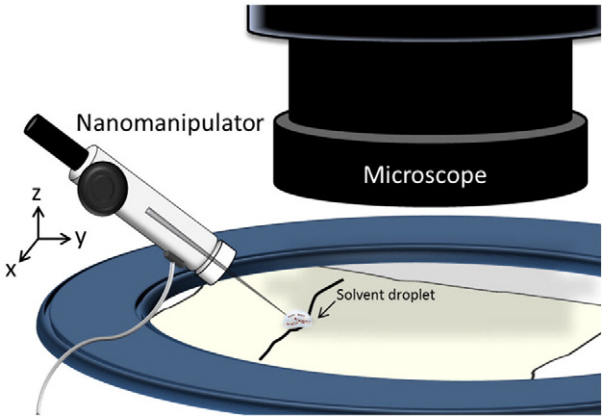

Fig. 1. Schematic of the nanomanipulator extracting ink from a document, movable in xyz-planes.

the document via cutting strips [12,15,16], micropunching holes [17], or extracting ink coated fibers [6] and then soaking those pieces into a solvent in order to remove the ink. These preconcentration techniques require longer sample preparation and analysis time. Mass spectrometric techniques such as matrix-assisted laser desorption ionization (MALDI) [18,19,20], secondary ion mass spectrometry (SIMS) [21], direct analysis in real time mass spectrometry (DART-MS) [22,23,24], desorption electrospray ionization (DESI) [25,26], and liquid extraction surface analysis (LESA) [27], laser ablation inductively coupled mass spectrometry (LA-ICP-MS) [28,29,30], SEM-EDS [31], and LIBS [15,29,30,32,33,34] are all direct analysis techniques with minimal to no sample preparation needed, saving time. One main issue arises when using these techniques, full document analysis without destruction cannot be achieved. MALDI, SIMS, LA-ICP-MS, and SEM-EDS can analyze documents without added destruction, but are confined to the limited size of the sample holder which eliminates full document analysis. DART-MS, DESI, and LIBS can directly analyze full documents but require a large amount of surface area for analyte ionization, making these techniques more destructive. Analyzing at trace levels is difficult for LIBS to achieve [29]. LESA has an enclosed workstation, constricting full document investigation, and utilizes a pipette tip with a diameter of 800 μm for sample extraction. This size pipette tip creates a wetted area of 1–3 mm which aids unnecessary harm to the document [35]. An assortment of methods so far has been used to distinguish between legal and counterfeit currency, but researching on a technique that preserves the integrity of the articles while conducting analyses is much needed.

Microscopy with direct analyte-probed nanoextraction coupled to nanospray ionization mass spectrometry (DAPNe-NSI-MS) is a direct extraction technique for analyzing ultra-trace amounts of material (as low as 300 attograms). This is made possible by equipping a nanomanipulator to the stage of a high-powered microscope. The nanomanipulator contains a piezoelectric-controlled nanopositioner with a removable nanospray tip (i.d. of 1 μm) to aspirate/extract via pressure injector shown in Fig. 1. DAPNe-NSI-MS has been used for the extraction of trace cocaine particles directly from a single rayon fiber [36], ultra-trace residues retrieved from electrostatic lifting process [37], the cleavage and extraction of peptides from resin beads [38], analyzing trace analysis of energetic materials [39], and the extraction of lipid contents directly from organelle preparations of plant tissues [40]. Recently, the DAPNe technique has proven its, direct extraction, analytical scheme for document and ink analysis by extracting ancient and modern inks from documents [41] and proving a document was falsified by identifying ink forgery [42]. DAPNe was coupled to fluorescence microscopy and Raman spectroscopy to identify where the forgery occurred within the text. The direct extraction scheme is conducted by placing a 2 μL solvent droplet onto the ink of interest, minimizing the surface area wetted to 5 μm or less post-extraction. The pre-filled nanospray tip is then positioned into the droplet, propelling a miniscule amount of solvent, inducing liquid phase microextraction. After the ink components diffuse into the droplet (15–20 s), it is then extracted into the tip for mass spectrometric analysis without further modification. By coupling NSI-MS with DAPNe, the resolution is increased and picomolar sensitivity is achieved. Coupling other techniques with DAPNe-NSI-MS opens the window for many opportunities beneficial for the scientific community. In this study, DAPNe-NSI-MS is coupled with laser ablation to analyze redacted documents.

Laser ablation is a technique that requires an infinitesimal or miniscule amount of sample preparation and is easy to learn and perform. Laser ablation has the ability to thwart attempts at redacting a document. This process is nondestructive and has fine control so that the settings can be changed for different media and inks. The application of laser ablation would be to strip the ink used to redact the document from the handwritten/typed text. This is possible due to the effects of multi-pass laser ablation over large areas and single lines of multiple layered inks which have been printed or written on paper. Steward et al. [43] multi-layered colored inks on white wood pulp paper to generate a full colored image with a tactile quality (creating features for anti-counterfeiting color copying). LA was used to effectively remove selective layers subsequently, revealing the different colored inks. The same technique was also efficiently applied when layering ink samples consisting of white/cyan/white/black layers [44]. LA is simple, rapid, with good precision, and almost harmless to the sample and is very suitable for the demand of pen analysis in forensic chemistry. Ma et al. [45] laser ablated 95 different blue ballpoint pens and almost no damage was done to the sample. The laser power and parameters were adjusted to remove just enough ink for metal analysis with no visible destruction. LA is a necessity when analyzing disguised or covered-up inks, exposing a small area for ink extractions. Furthermore, it is questionable whether the ink used to redact the text suppresses the oxidation of the handwritten/printed ink underneath and whether the ink chemistry of the underlying text is further oxidized by the effects of the laser. By tracking the oxidation process, these questions can be elucidated. This paper will demonstrate that the laser ablation process is successful for inkjet printed and handwritten documents; in combination with the proven techniques of nanomanipulation extraction for further analysis. With this, the oxidation process of the handwritten/typed text concealed can be determined.

2. Materials and methods

2.1. Reagents and solvent preparation

All solutions were made with Millipore water, obtained from Aqua Solutions Inc. (Deer Park, TX) having 18 MΩ resistivity. The glacial acetic acid was purchased from Mallinckrodt Baker Inc. (Phillipsburg, NJ). Optima LC/MS methanol, acetonitrile, toluene, chloroform, ammonium hydroxide, and analytical grade ammonium acetate were acquired from Fischer Scientific (Fair Lawn, NJ). A deskjet ink cartridge (HP 60 Black Noir) and laserjet cartridge (HP 43× black toner) was obtained from Hewlett-Packard Company (Palo Alto, CA). Uni-Ball black ballpoint pen, a black Sharpie permanent marker, BIC pens, Pilot pens, Expo markers, and Casemate permanent marker were commercially purchased.

Several solvents were used to optimize the extraction of inks, including chloroform, acetonitrile, methanol, and toluene. Acetonitrile and methanol were optimal for ballpoint pen ink extraction and acetonitrile was optimal for deskjet printed ink extraction. It is important to note that none of the listed solvents were able to extract any compounds from laser printed paper (data not shown). This may be because the laser printer uses toner-based cartridges instead of ink-based cartridges.

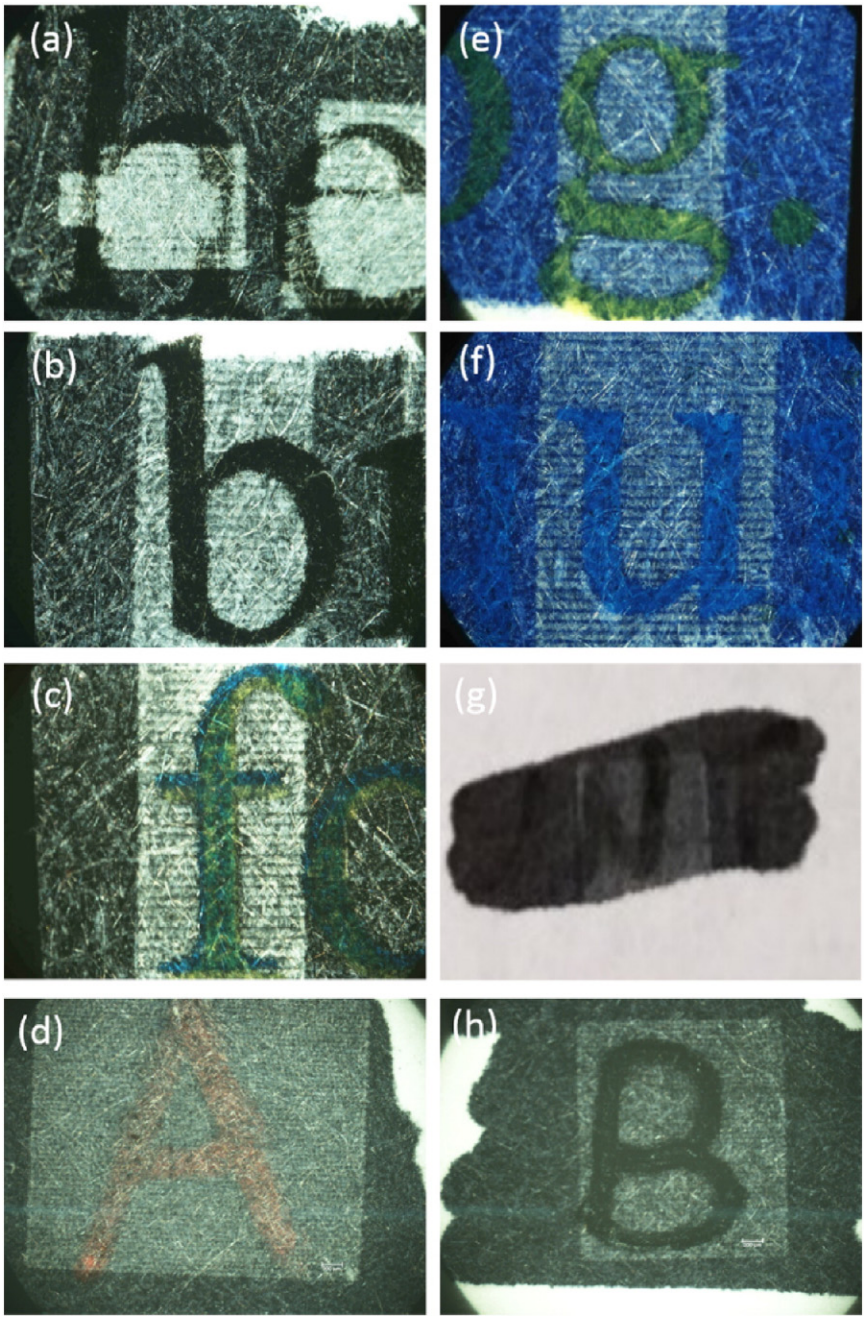

Fig. 2. An illustration of redacted ink, post-laser ablation where (a) shows what the sample would look like with poor LA settings of black printed text redacted with a black Sharpie, (b) is black printed text redacted with black Sharpie, (c) is green printed text redacted with black Sharpie, (d) is handwritten red (BIC) ink redacted with permanent marker (Casemate), (e) is yellow printed text redacted with blue Sharpie, (f) is blue printed text with blue Sharpie, (g) is handwritten black ink (Uni-ball) redacted with black Sharpie, and (h) is handwritten black (Pilot) ink redacted with black marker (Expo).

The extraction solvent for the ballpoint pen ink consisted of methanol:water (1:1, *v*/v) with 1% acetic acid and acetonitrile:water (1:1, *v*/v) with 0.1% ammonium acetate, separately. The inkjet printer ink extraction solvent used was made up of acetonitrile:water with 0.1% ammonium acetate. These solvents were used in conjunction with Millipore water (the solvent droplet) during the liquid phase microextraction.

2.2. Instrumentation

A L200 nanomanipulator (Zyvex; Richardson, TX), fixed onto the stage of a Nikon AZ 100 microscope (Nikon Instruments Inc.; Melville, NY), is controlled by maneuvering the removable nanospray tip via joystick controller (fine spatial resolution up to 5 nm). A PE2000b four channel pressure injector (MicroData Instruments Inc.; S. Plainfield, NJ) controls the aspiration/extraction of the nanospray tip. All mass spectrometric analyses were conducted on a LCQ DECA XP Plus equipped with a nanospray ionization source (Proxeon Biosystems; Odense, Denmark). After the sample extraction is complete, the nanospray tip is removed from the nanomanipulator and transferred directly to the nanospray ionization source with no further alteration. The nanomanipulator has been previously detailed [40–42,44,46,47] and the direct analytical scheme used for the extraction of ink from documents is described thoroughly by Huynh et al. [41,42].

A UP-213 laser ablation instrument (New Wave; Freemont, CA) with a 213 nm Nd:YAG laser source was used to perform the ablation of the

Table 1
Laser setting differences between handwritten and printed texts for redacted documents.

Parameters	Handwritten text	Printed text
Raster spacing	100 μm	100 μm
Raster speed	100 μm/s	100 μm/s
Spot size	100 μm	100 μm
Output	60%	60%
Repetition rate	1 Hz	4 Hz
Flow rate	50 mL/min	50 mL/min
Number of passes	2	1

redacted handwritten and printed documents. The samples were written/printed on generic multipurpose computer paper. Five samples of each (handwritten and printed text) were created and redacted with a Sharpie permanent marker at the same time, labeled day 0 to day 4. Fig. 2 shows examples of the different samples that were redacted post laser ablation. Fig. 2a shows an example of a sample that was poorly laser ablated. Fig. 2(b–h) are variations of different redacted inks laser ablated with optimized settings. A redacted sample and a control sample were examined. The control sample was not redacted. The prepared sample text was marked over until the paper was highly saturated with the redacting marker ink. Day 0 redacted sample was then placed into the ablation chamber with 50 mL/min of argon gas to provide an inert and dry environment, and additionally clearing away any ablated material. Methods were developed for various materials with minor differences exhibited between sample types, Table 1. Fig. 2(d) and (h) used different markers to redact the underlying text, using 85% laser power instead of 60% with one pass. The ablation process was repeated every 24 h for 5 consecutive days.

2.3. Direct extraction analytical scheme

The nanospray tip is filled with the desired extraction solvent prior to insertion into the nanopositioner. A 2 μL droplet of Millipore water is dispensed onto the ink. The nanospray tip is then positioned into the solvent droplet and aspirated with a miniscule amount of extraction solvent using an injection pressure of 15 psi and allowed to sit for 15–20 s, letting the ink diffuse into the droplet. It is important to note that propelling the extraction solvent into the water droplet encourages liquid phase microextraction, allowing the components of ink to dissolve into the droplet. The droplet is finally extracted from the page with a fill pressure of 35 psi. The analyte contained in the nanospray tip is directly analyzed through NSI-MS without further modification.

2.4. Oxidation of redacted inks

The inkjet printed text, laser printed text, and handwritten ink was redacted as soon as the ink was dried (30 min—1 h). Five replicates of each sample were made, kept in a case, and stored in a desk drawer throughout the experiments. Each sample was laser ablated and then the ink was extracted for spectrometric analysis for five consecutive days. The first sample was completed directly after it was redacted, known as day 0. Oxidation was then quantified by calculating the percent relative peak area (RPA) with three repetitions. Mass spectra were scanned from a range of *m/z* 50–1500 in positive mode at 2.5 kV.

2.5. Oxidation effects of laser ablation on inks

The effect of laser ablation on written ink, that has not been redacted, has been investigated. The ultraviolet (UV) radiation and plasma heating of the laser could potentially oxidize the hidden text underneath further while removing the Sharpie layer. A Uni-ball black pen was used to draw several lines. Each line of ink was laser ablated at different laser powers ranging from 0 to 100% at 1 Hz. Once the ink line was laser ablated at a set power, DAPNe-NSI-MS was used to extract the ink and monitor the oxidation of PEG peaks by calculating the RPA.

3. Results and discussion

3.1. Oxidation of polyethylene glycol

Ballpoint pens with oil-based inks were first introduced in the 1940s, presenting a new kind of writing apparatus and ink. Before this time, water-based inks were used with fountain and dip pens [47]. Polyethylene glycol (PEG)-based inks began replacing the oil-based ink formulas in 1952. Advancing through history, many different pen apparatuses and ink formulas were introduced; but PEG has managed to remain constant in many ink formulations today. The polar nature of PEG has allowed a wider range of dyes to be used and were found to adhere firmly to cellulose fibers where inks can neither be smudged nor transferred [48]. It also helps pigments to stay dispersed in solution. The molecular structure of PEG contains a repeating oxyethylene unit (–C_2H_4O—), making the oligomer distribution spaced 44 u apart [49]. The structural formula of PEG is $H(C_2H_4O)_nOH$, where n represents the number of repeating units. For mass spectral analysis, PEG ions are observed to have proton, sodium, or potassium adducts, $[HO(C_2H_4O)_nH + H]^+$, $[HO(C_2H_4O)_nH + Na]^+$, or $[HO(C_2H_4O)_nH + K]^+$, respectively [7].

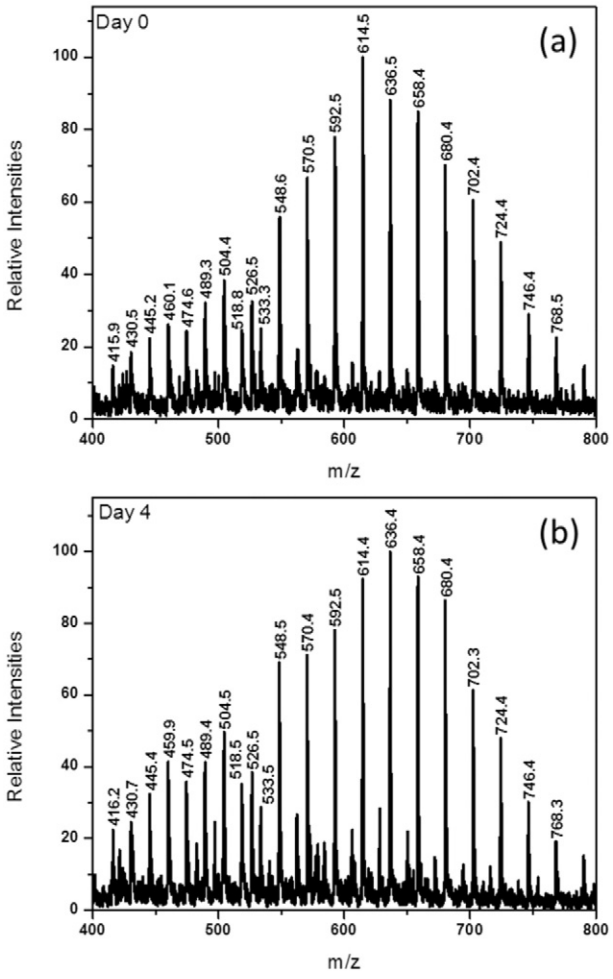

Fig. 3. The spectrum obtained when extracting printer ink with acetonitrile:H_2O (1:1) with 0.1% ammonium acetate where (a) was characterized on day 0 and (b) was characterized on day 4.

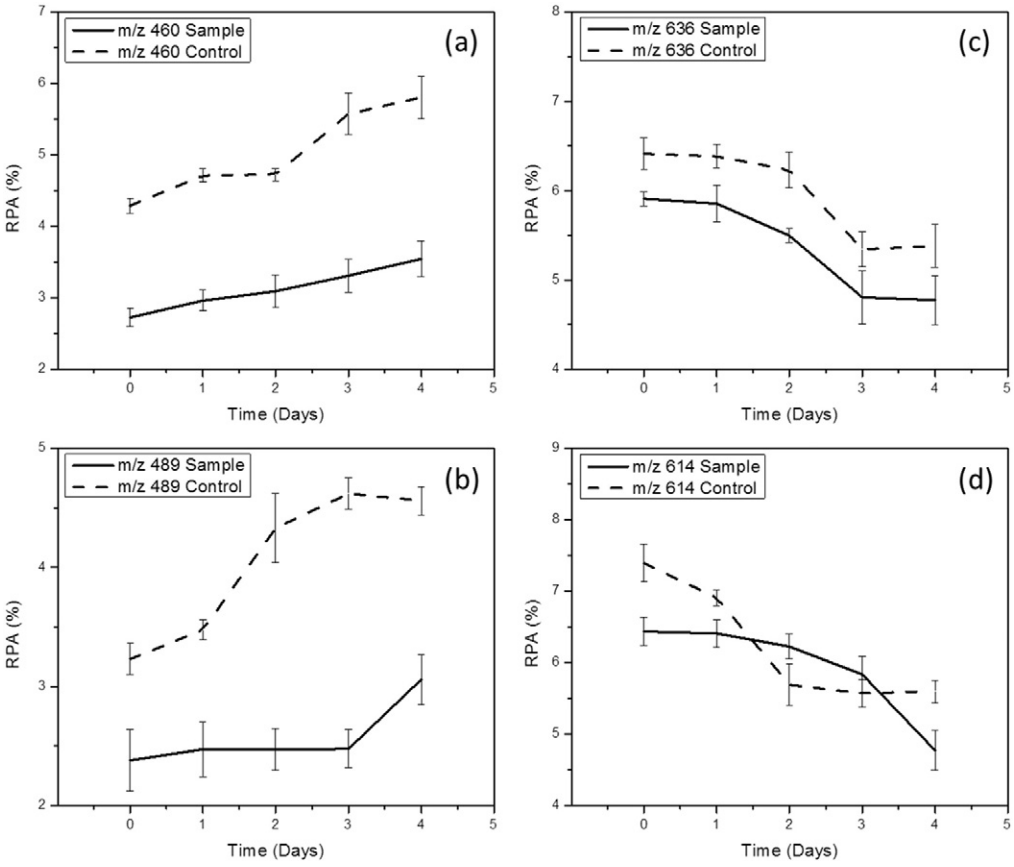

Fig. 4. RPA (%) curves depicting the oxidation of deskjet printer ink over five days.

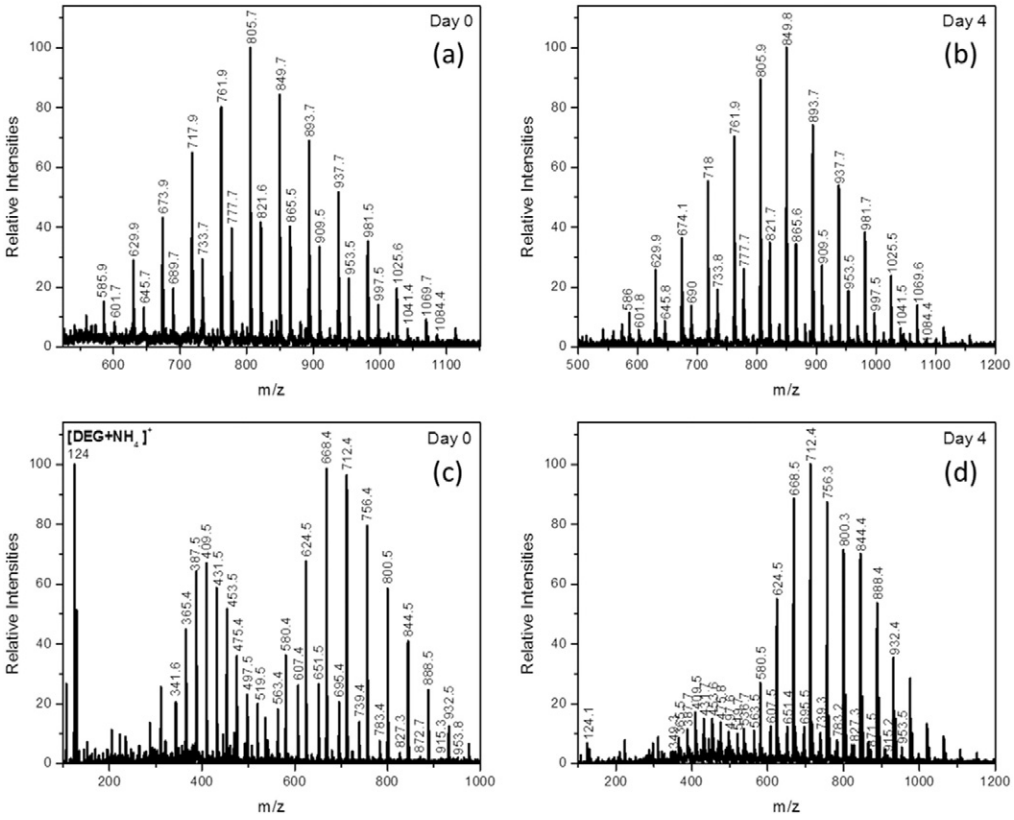

Fig. 5. The spectra of Uni-ball black pen where (a, b) were extracted with methanol:H_2O with 1% acetic acid on day 0 and day 4 and (c, d) were extracted with acetonitrile:H_2O with 0.1% ammonium acetate on day 0 and day 4 using DAPNe-NSI-MS.

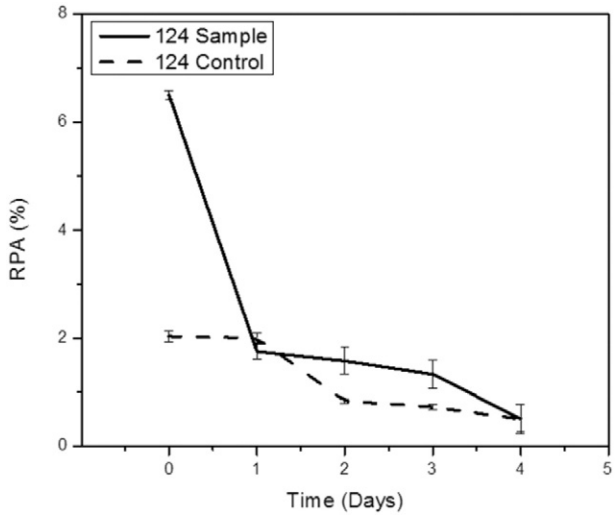

Fig. 6. RPA (%) curve depicting the oxidation of DEG within Uni-ball black pen over five days when extracting with acetonitrile:H_2O with 0.1% ammonium acetate.

Unfortunately, PEG is susceptible to radical oxidative attack. This leads to the thermal degradation of PEG producing low molecular weight products. As thermal degradation continues, the amount of low molecular weight products increase [50]. L. Boughen et al. [51] determined that after a few years of PEG in a capped bottle, the degraded PEG had a strong aldehyde/ketone odor and it had become a paste (like toothpaste). J. Glastrup et al. [52] heated PEG 4000 for 2–4 h which has in some cases led to the formation of a liquid that would not solidify after cooling. They have shown that this liquid more resembled PEG 600 than the original PEG 4000. For those valuable reasons, the relative peak area (RPA) equation may be implemented to track the oxidative process of polyethylene glycol, and is defined as:

$$\mathrm{RPA}_i = \frac{A_i}{A_{tot}} \times 100\%$$

where A_i is the area of peaks of interest at $m/z = i$ and A_{tot} is the summation of all the significant signals above a certain intensity threshold [8,15,41,42,53]. The overall concentration cannot be controlled, but relative amounts of extracted analytes are consistent within a given extraction solvent.

3.2. Oxidation of printer inks

Shown in Fig. 3, three polymeric distributions have been extracted from a deskjet printed text simultaneously. The low molecular weight distribution, including peaks m/z 415.9, 430.5, 445.2, 460.1, 474.6, 489.3, 504.4, 518.8, and 533.3, are derived from a polymer known as polymethylene. Each of those peaks are spaced 14 u with the structural formula of $(-CH_2-)_n$ [54]. The high molecular weight distribution, including peaks m/z 526.5, 548.6, 570.5, 592.5, 614.5, 636.5, 658.4, 680.4, 702.4, 724.4, 746.4, and 768.5, are separated by 22 u between each peak and 44 u between every other peak. This contains two homologous PEG distributions within itself.

The oxidation trend, after five days, correlates with the degradation studies of PEG [50–52]. As thermal degradation progresses after each day, the amount of low molecular weight products increase, causing the melting point and heat of fusion to be lowered [50]. A shift in peak

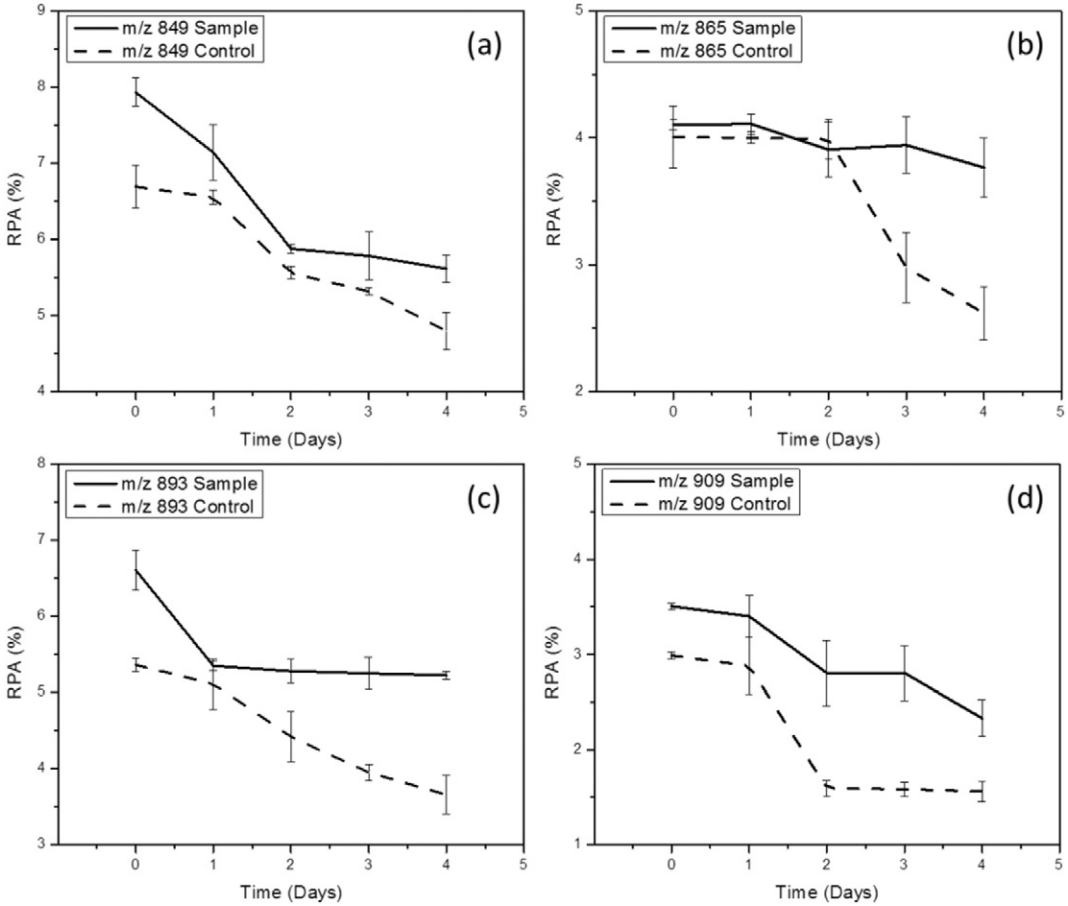

Fig. 7. RPA (%) curves depicting the oxidation of Uni-ball black pen over five days when extracting with methanol:H_2O with 1% acetic acid.

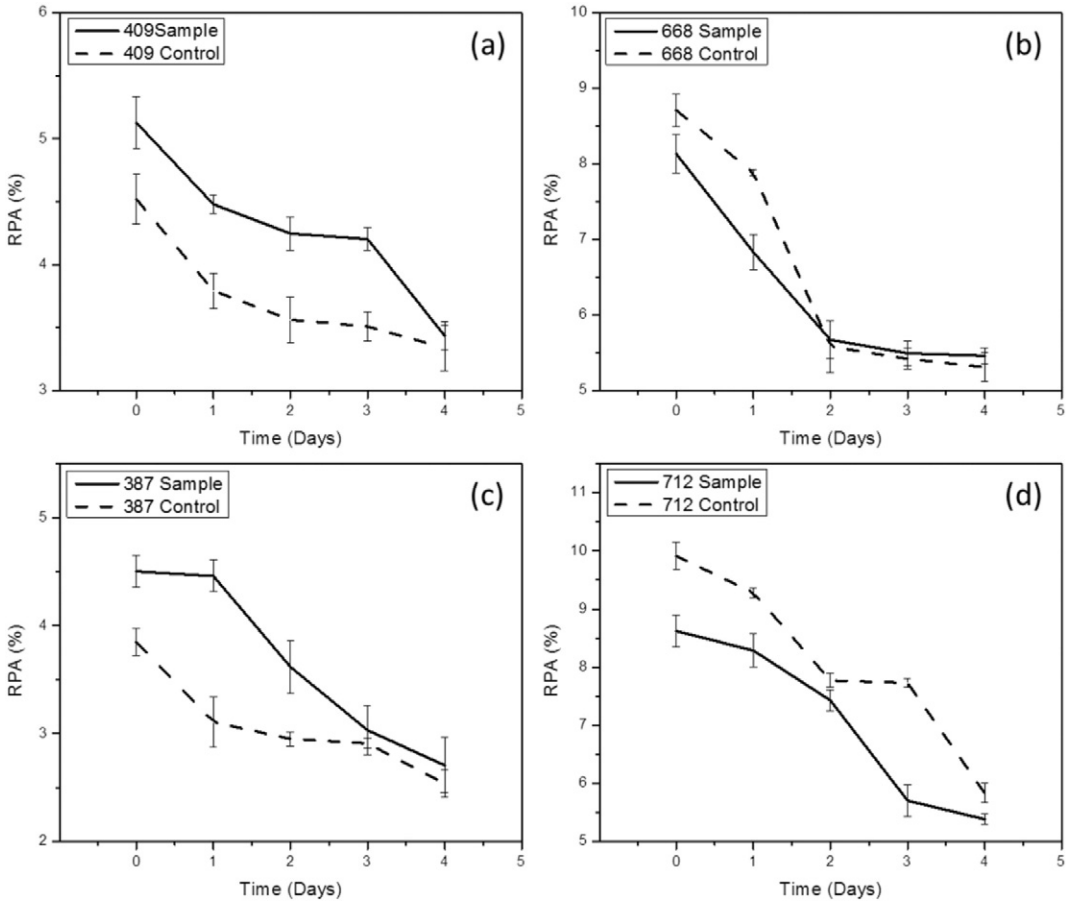

Fig. 8. RPA (%) curves depicting the oxidation of Uni-ball black pen over five days when extracting with acetonitrile:H_2O with 0.1% ammonium acetate.

intensities is observed after five days (day 0 to day 4), shown in Fig. 3. For example, peak *m/z* 614.5 is no longer the most abundant peak; over time, peak *m/z* 636.4 becomes the most abundant peak. The oxidation progress of peaks *m/z* 460, 489, 636, and 658 was quantitated by calculating the RPA (%) values shown in Fig. 4. It is imperative to acknowledge any peak may be observed and that there is no significance in the specific peaks that were chosen. The general trend for the larger peaks, *m/z* 614 and 636, progressively decreases. The high molecular weight peaks are thermally degrading, increasing the intensities of the low molecular weight peaks. This is proven by the increase in RPA (%) when monitoring the following low molecular weight peaks, *m/z* 460 and 489, and the decrease in high molecular weight peaks, *m/z* 614 and 636. The controls in Fig. 4(a, b) begin at higher RPA (%) values than the samples. This is because the controls for the high molecular weight peaks are oxidizing at a faster rate than the once redacted samples. The faster oxidation rate produces more low molecular weight products. This difference may be due to the masking effect of the Sharpie permanent marker.

3.3. Oxidation of ballpoint pen

The DAPNe technique can facilitate the chemical variations of ink by changing the extraction solvent. Fig. 5 illustrates the different spectra obtained when extracting with two different solvents. The extraction solvent used in Fig. 5(a, b) was methanol:H_2O (1: 1) with 1% acetic acid, where polyethylene glycol was the main component removed. Two distributions were observed. The outer distribution, including peaks *m/z* 585.9, 629.9, 673.9, 717.9, 761.9, 805.7, 849.7, 893.7, 937.7, 981.6, 1025.6, and 1069.7, are PEG ions with sodium adducts ($[M + Na]^+$, where M represents the molecular species). The inner distribution, including peaks *m/z* 601.7, 645.7, 689.7, 733.7, 777.7, 821.6, 865.5, 909.5, 953.5, 997.5, 1041.4, and 1084.4, are PEG ions with potassium adducts ($[M + K]^+$). The difference between the adjacent peaks are 16 u (e.g., *m/z* 805.7 and 821.6), which correlates with the difference between sodium and potassium mass units. A. Anne et al. [55] observed the same phenomenon when analyzing modified PEG using a MALDI-TOF spectrometer where the potassium adducts were part of the inner distribution and the sodium adducts were part of the outer distribution. The spectra shown in Fig. 5 (c, d) was obtained by extracting the Uni-ball black pen using acetonitrile:H_2O (1:1) with 0.1% ammonium acetate. Three different polymer distributions were obtained as well as diethylene glycol (DEG). DEG is a moist-keeping agent and also a volatile vehicle component that is anticipated to carry the dye or pigment onto the writing surface, increasing the bond strength between the ink and writing surface [2]. The peak at *m/z* 124 represents DEG with an ammonium ion adduct, $[DEG + NH_4]^+$. The same peak was observed when J. Ding et al. [56] analyzed diethylene glycol in toothpaste products using neutral desorption reactive extractive electrospray ionization tandem mass spectrometry. The affinity of the cation adduct was studied, concluding that the DEG molecules have a higher affinity towards forming a complex with an ammonium cation than with a sodium cation. For this reason, $[DEG + Na]^+$ complex does not form a significant

$$HOCH_2CH_2OH + n(CH_2CH_2O) \Longrightarrow HO(CH_2CH_2O)_{n+1}H$$

Fig. 9. Polymerization of ethylene oxide with ethylene glycol forming PEG.

Table 2
The calculations for the Δ[]/Δt from the RPA (%) curves.

Experiment	Concentration (RPA)	Initial rate (RPA/s)
Peak *m/z* 614 control, degradation		
Day 0–1	0.0738–0.0691 = 0.0047	5.44×10^{-8}
Day 1–2	0.0691–0.0573 = 0.0118	1.37×10^{-7}
Day 2–3	0.0573–0.0571 = 0.0002	2.31×10^{-9}
Day 3–4	0.0571–0.0560 = 0.0011	1.27×10^{-8}
Peak *m/z* 614 sample, degradation		
Day 0–1	0.0644–0.0643 = 0.0001	1.16×10^{-9}
Day 1–2	0.0643–0.0622 = 0.0021	2.43×10^{-8}
Day 2–3	0.0622–0.0583 = 0.0039	4.51×10^{-8}
Day 3–4	0.0583–0.0476 = 0.0107	1.24×10^{-7}
Peak *m/z* 636 control, degradation		
Day 0–1	0.0641–0.0637 = 0.0004	4.63×10^{-9}
Day 1–2	0.0637–0.0623 = 0.0014	1.62×10^{-8}
Day 2–3	0.0623–0.0538 = 0.0085	9.84×10^{-8}
Day 3–4	0.0538–0.0536 = 0.0002	2.32×10^{-9}
Peak *m/z* 636 sample, degradation		
Day 0–1	0.0591–0.0586 = 0.0005	5.79×10^{-9}
Day 1–2	0.0586–0.0550 = 0.0036	4.17×10^{-8}
Day 2–3	0.0550–0.0480 = 0.0070	8.10×10^{-8}
Day 3–4	0.0480–0.0477 = 0.0003	3.47×10^{-9}
Peak *m/z* 658 control, degradation		
Day 0–1	0.0570–0.0570 = 0.0000	0
Day 1–2	0.0570–0.0562 = 0.0008	9.26×10^{-9}
Day 2–3	0.0562–0.0462 = 0.0100	1.16×10^{-7}
Day 3–4	0.0462–0.0458 = 0.0004	4.63×10^{-9}
Peak *m/z* 658 sample, degradation		
Day 0–1	0.0565–0.0554 = 0.0011	1.27×10^{-8}
Day 1–2	0.0554–0.0541 = 0.0013	1.50×10^{-8}
Day 2–3	0.0541–0.0537 = 0.0004	4.63×10^{-9}
Day 3–4	0.0537–0.0493 = 0.0044	5.09×10^{-8}
Peak *m/z* 460 control, formation		
Day 0–1	0.0472–0.0429 = 0.0043	4.98×10^{-8}
Day 1–2	0.0473–0.0472 = 0.0001	1.16×10^{-9}
Day 2–3	0.0557–0.0473 = 0.0084	9.72×10^{-8}
Day 3–4	0.0578–0.0557 = 0.0021	2.43×10^{-8}
Peak *m/z* 460 sample, formation		
Day 0–1	0.0295–0.0273 = 0.0022	2.54×10^{-8}
Day 1–2	0.0310–0.0295 = 0.0015	1.74×10^{-8}
Day 2–3	0.0331–0.0310 = 0.0021	2.43×10^{-8}
Day 3–4	0.0354–0.0331 = 0.0023	2.66×10^{-8}
Peak *m/z* 474 control, formation		
Day 0–1	0.0404–0.0368 = 0.0036	4.17×10^{-8}
Day 1–2	0.0469–0.0404 = 0.0065	7.52×10^{-8}
Day 2–3	0.0507–0.0469 = 0.0038	4.40×10^{-8}
Day 3–4	0.0511–0.0507 = 0.0004	4.63×10^{-9}
Peak *m/z* 474 sample, formation		
Day 0–1	0.0277–0.0222 = 0.0055	6.37×10^{-8}
Day 1–2	0.0288–0.0277 = 0.0011	1.27×10^{-8}
Day 2–3	0.0290–0.0288 = 0.0002	2.31×10^{-9}
Day 3–4	0.0332–0.0290 = 0.0042	4.86×10^{-8}
Peak *m/z* 489 control, formation		
Day 0–1	0.0348–0.0324 = 0.0024	2.78×10^{-8}
Day 1–2	0.0434–0.0348 = 0.0086	9.95×10^{-8}
Day 2–3	0.0462–0.0434 = 0.0028	3.24×10^{-8}
Day 3–4	0.0462–0.0459 = 0.0003	3.47×10^{-9}
Peak *m/z* 489 sample, formation		
Day 0–1	0.0247–0.0238 = 0.0009	1.04×10^{-8}
Day 1–2	0.0247–0.0247 = 0.0000	0
Day 2–3	0.0247–0.0247 = 0.0000	0
Day 3–4	0.0306–0.0247 = 0.0059	6.83×10^{-8}
Incandescent light, peak *m/z* 801		
0–4 h	0.1477–0.1463 = 0.0014	1.62×10^{-8}
4–8 h	0.1463–0.1146 = 0.0317	3.67×10^{-7}
8–12 h	0.1146–0.0668 = 0.0478	5.53×10^{-7}
12–16 h	0.0668–0.0691 = 0.0023	2.66×10^{-8}
16–20 h	0.0691–0.0700 = 0.0009	1.04×10^{-8}
20–24 h	0.0700–0.0372 = 0.0328	3.80×10^{-7}

amount when extracting the Uni-ball pen with methanol:H_2O (1:1) with 1% acetic acid. The peaks in the first polymeric distribution are spaced 22 u apart, including peaks at *m/z* 341.6, 365.4, 387.5, 409.5, 431.5, 453.5, 475.4, 497.5, and 519.5. Once again, this is due to two homologous PEG distributions, where every other peak is separated by 44 u. The two remaining distributions, overlapping, are PEG. These peaks are separated by 44 u and the adjacent peaks have a difference of 16 u, concluding PEG complexes with sodium and potassium adducts are present [7].

Oxidation can be observed through the peak shifts just after five days and by the obvious change in ratios between the DEG complex and the polymeric distributions (Fig. 5(c, d)). DEG is a volatile organic component where a majority of its disappearance occur as soon as the ink is deposited on the writing surface. The RPA (%) curves shown in Fig. 6, shows that redacting the text was effective. The control starts at a lower RPA (%) value because most of the DEG had already volatized compared to the sample. There is a 4.47 ± 0.01% difference between the control and sample on day 0. The time it took to write the text to the time it took to implement the first extraction, 1–2 h, most of the volatiles had already disappeared. Redacting the text caused the sample to have a higher RPA (%) value compared to the control. The volatiles in the masked ink were temporarily suppressed, especially between day 0 and day 1. All the RPA (%) curves in Fig. 7 are decreasing. The sample RPA (%) curves begin at a higher value, signifying that the redaction process was also effective. The RPA (%) curves for peaks *m/z* 387, 409, 668, and 712 are all thermally degrading, explaining the decreasing trend seen in Fig. 8. Redacting the document has also shown to be effective due to the sample peaks having higher RPA (%) values.

3.4. Kinetics

For inks, the environment has a huge impact on how the ink in the pens oxidize. By calculating the kinetics at which these reactions occur, we can determine the reaction rates and overall order with respect to the changing environment (i.e., heating with an incandescent bulb and redacting the text). The different chemistry that occurs during the oxidation of inks leads to some components degrading into products while some of those products simultaneously polymerize to form larger products.

The low molecular weight products during oxidation include formaldehyde, acetaldehyde, formic acid, acetic acid, diethylene glycol, triethylene glycol, tetraethylene glycol, and ethylene glycols. The major products formed are formic acid and ethylene glycol. Due to radical oxidative attack, glycol oxides are also formed. These products also polymerize into PEG chains [57].

$$[PEG]_n + O_2 \rightarrow \text{low molecular weight products [aldehydes + organic acids]}$$

Moreover, ethylene oxide can polymerize with glycol derivatives, via radical and ionic mechanisms, and form PEG. This produces smaller chains from the initial PEG structure shown in Fig. 9.

PEG is produced by the interaction of ethylene oxide with water, ethylene glycol, or ethylene glycol oligomers. The condensation of PEG is not limited to the interaction of ethylene oxide, but to other glycol oxides as well. The reaction rate of the degradation and formation of PEG can be determined through kinetics as well as the reaction order. For simplicity variables are used, as follows:

$$\text{Degradation}: [A]^a + [B]^b [C]^c$$

$$\text{Formation}: [C]^c \xrightarrow{k_3} [D]^d$$

A represents PEG, B represents excess oxygen, C signifies one of the low molecular weight products formed which are glycol oxides, and D refers to the polymerization product from glycol oxides. The concentration of PEG is the only reactant that changes over time. This is because the

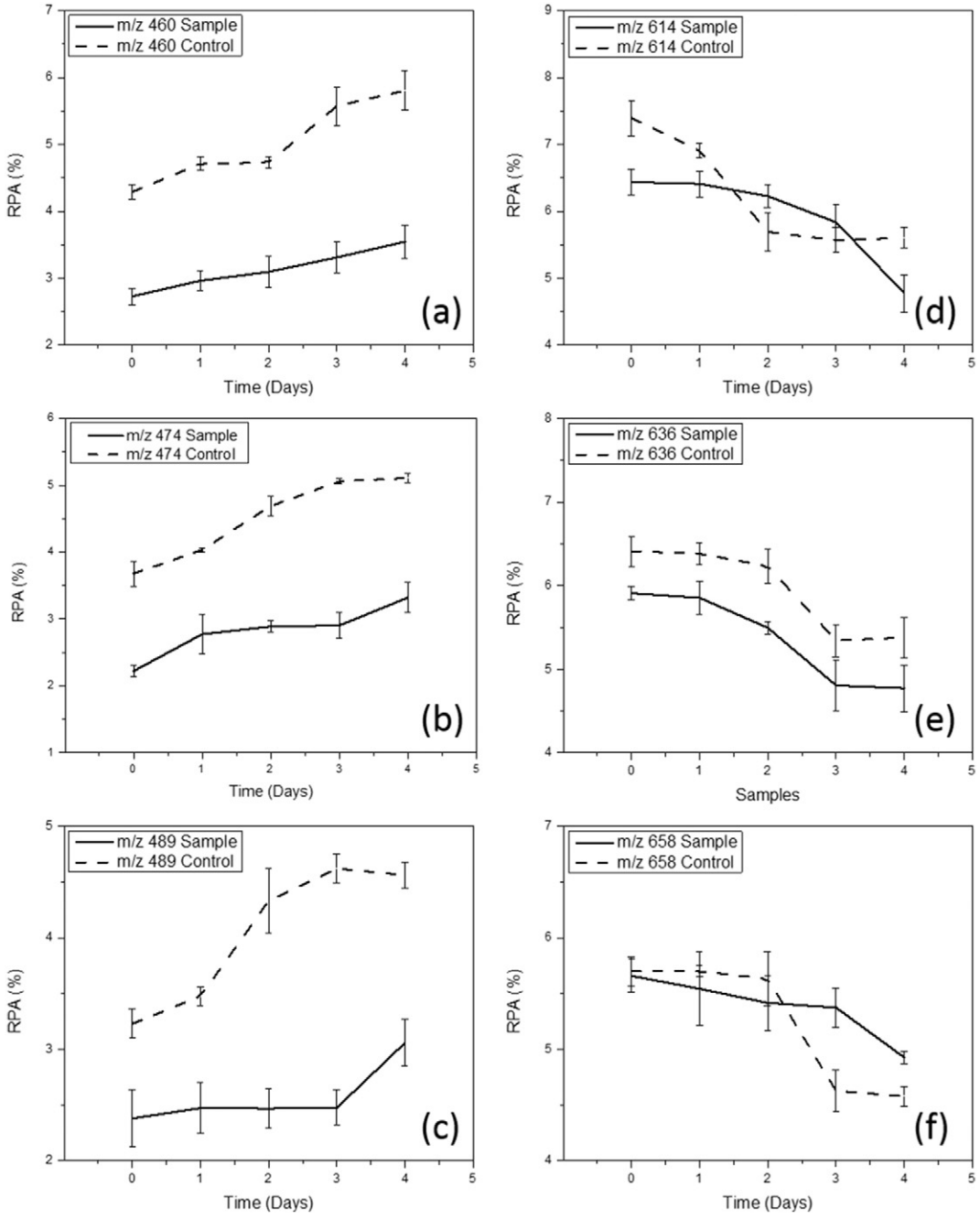

Fig. 10. RPA (%) curves monitoring the oxidation of PEG of individual peaks where (a–c) are the low molecular weight peaks and (d–f) are the high molecular weight peaks.

concentration of O_2 is in excess and does not change to any appreciable amount. Thus, a method of flooding or method of isolation was implicated on the final rate law in order to derive the final equation:

$$\text{Rate}_D = k'[A]^a \quad (1)$$

where $k' = \frac{k_3 k_1 [B]^b}{k_2 + k_3}$ and $[B]^b$ has been included as a constant in the reaction. In order to determine the reaction order, values from Table 2 must be plugged into the Rate_D equation. The values were obtained by calculating the $\frac{\Delta[]}{\Delta t}$ per day from the RPA (%) curve (Fig. 10). The RPA (%) represents the reactants decreasing over time when exposed to air as well as products polymerizing and forming new peaks. By inserting the values from Table 2 into Eq. (1), first order kinetics is obtained for all values. For example,

$$\frac{\text{Rate}_{D2}}{\text{Rate}_{D1}} = \frac{\left[k'[A]^a\right]_2}{\left[k'[A]^a\right]_1}$$

$$\frac{2.78\text{x}10^{-8}}{2.43\text{x}10^{-8}} = \frac{0.0024^a}{0.0021^a}$$

$$1.14 = \left[\frac{0.0024}{0.0021}\right]^a$$

$$1.14 = 1.14^a$$

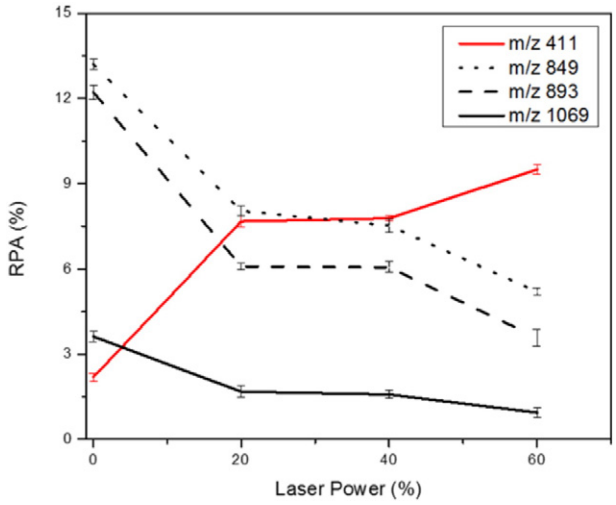

Fig. 11. RPA (%) curves of individual peaks from PEG obtained from the extraction of ink laser ablated at different powers.

Therefore, "a" must equal 1 concluding first order kinetics. In the application of redacted documents, the reaction rate does not differ more than one order of magnitude. In the case where the ink is exposed to incandescent heat exposure, the initial rate of reaction occurs more than one order of magnitude faster compared to ink exposed to air. Although the reaction rate is faster, the order stays consistent.

3.5. Oxidation effects of laser ablation on inks

The high plasma temperature and plasma expansion induced from laser ablation could potentially have an effect on the underlying text. It is important to note the possible chemical changes and degradation of the ink caused by the interaction of the laser during the removal of the redacted layer. In order to show this effect, the written text itself (not redacted) was laser ablated at different energies to see how its profile oxidizes with increasing power. Fig. 11 shows this effect by laser ablating, a drawn ink line, at different laser powers ranging from 0 to 100%. The high molecular weight peaks from PEG such as *m/z* 849, 894, and 1069 are decreasing as the low molecular weight peak such as *m/z* 411 is increasing. The largest oxidation change was observed between 0% laser power (fresh ink) and 20% laser power where peaks *m/z* 411, 849, 893, and 1069 showed a 5.48 ± 0.06%, 5.08 ± 0.03%, 6.123 ± 0.09%, and 1.94 ± 0.02% difference respectively. A significant change was not detected after 20% laser power was used. The largest alteration distinguished between 20 and 40% was 0.52 ± 0.05% for *m/z* 849. Between 40% and 60% laser power, the RPA values had a difference of 1.72 ± 0.05%, 2.32 ± 0.07%, 2.48 ± 0.07%, 0.64 ± 0.01% for peaks *m/z* 411, 849, 893, and 1069. The fourth highest molecular weight peak, *m/z* 1069, almost disappeared after implementing 60% laser power on the ink (0.94 ± 0.16% remaining). When laser ablating the inks with 80 and 100% power, there was not enough ink left for extraction. Thus, PEG was not seen in the spectra.

A laser power of 60% was used to remove the redacting ink layer from the text. As shown in Fig. 2, the Sharpie was not completely removed but enough was removed to clearly reveal the text that was once redacted and to extract the underlying ink. Fig. 7 shows the effect of the laser on day 0 between the control and the sample. These samples were created at the same time where the control was not redacted and the sample was redacted with a Sharpie. After laser ablating and analyzing the sample, peaks *m/z* 849 and 893 has a 1.24 ± 0.06% and 1.25 ± 0.12% difference, respectively, between the sample and the control on day 0. This indicates that redacting the text and using laser ablation to remove the redacting ink affects the oxidation of the underlying ink by the aforementioned percentages. From this data, the Sharpie absorbs a majority of the UV radiation and plasma heating from the interaction of the laser but the underlying ink is still mildly affected.

4. Conclusion

Redacting documents or concealing text with another ink has been proven to influence the aging process of ink. Once ink is deposited on the writing surface, it will immediately start to age and oxidize. The aging process of ink can be altered in several ways. The "freshness" of the ink may differ depending on the surrounding levels of humidity and temperature. Ink may appear aged if heat was applied, such as setting the document in the sun or applying incandescent heat. Unfortunately, the drawback for applying laser ablation to full documents is time. In order to ablate an area of 1 cm^2 with 100 μm spot size would take 2.78 h. Although effective, time would be an issue. Another issue to consider is the exposure of UV radiation and heat created between the laser and the ink, especially when monitoring the oxidation process of the ink. When the written text itself was laser ablated at 60% laser power, the RPA of the ink oxidized between 5–6%. The written text oxidized significantly less when redacted, the RPA changed about 1.25%. This deviation in RPA values could be compensated by using a correction factor (e.g., 1.25%) for a more accurate value. One last subject to consider when analyzing redacted documents is the chamber. The laser ablation chamber needs to be large enough to analyze full documents. This can be done by modifying the chamber to the desired size, which has been discussed in previous articles for different applications [58,59,60,61].

For future applications, the laser ablation method can also be used to distinguish between legitimate and counterfeit breeder documents such as a driver's licenses. Breeder documents, such as birth certificates with limited or poor security features, are used to acquire other forms of identification and if a criminal obtains a breeder document then they can assume another person's identity and participate in illicit activities while going undetected [62]. A plastic polymer is applied over printed identification cards and licenses. The plastic polymer interferes and prevents spectroscopy techniques from being utilized. By utilizing the laser ablation method the plastic polymer layer is ablated away and techniques such as Raman spectroscopy and DAPNe can be performed without opposition from the plastic polymer. Once a small section of the plastic is removed the laser will continue to ablate until the ink is exposed. Nanomanipulative techniques allow further chemical analysis and determining whether the original ink is being used on a falsified document. It can also be used to determine the ratio components in different inks, where the formulation is proprietary to the company. Overall, DAPNe-NSI-MS is very adaptable especially when coupled with other techniques which extends the window for many possibilities beneficial for forensic investigations. Furthermore, analyzing redacted documents from the federal government or documents from businesses are made easier with these techniques. By utilizing DAPNe-NSI-MS, the oxidation process can be monitored as well as characterizing the ink itself. Most importantly, the application of laser ablation and DAPNe is not harmful to the document, specifically the ink of interest.

Acknowledgements

This research is funded by the National Institute of Justice grant, award NIJ-2013-3361. We would also like to thank Gabriel Watts for his expertise, forensic document examiner with the U.S. Government.

References

[1] S. Bell, A Dictionary of Forensic Science, Oxford University Press, Oxford, 2012 http://dx.doi.org/10.1093/acref/9780199594009.001.0001.
[2] R. Brunelle, C. K., Advances in the Forensic Analysis and Dating of Writing Ink, Charlies C. Thomas Publisher, LTD., Springfield, 2003.
[3] J. Coumbaros, K.P. Kirkbride, G. Klass, W. Skinner, Application of time of flight secondary ion mass spectrometry to the in situ analysis of ballpoint pen inks on paper, Forensic Sci. Int. 193 (2009) 42–46, http://dx.doi.org/10.1016/j.forsciint.2009.08.020.

[4] B. Matthews, G.S. Walker, H. Kobus, P. Pigou, C. Bird, G. Smith, The analysis of dyes in ball point pen inks on single paper fibres using laser desorption ionisation time of flight mass spectrometry (LDI-TOFMS), Forensic Sci. Int. 209 (2011) e26–e30, http://dx.doi.org/10.1016/j.forsciint.2011.03.033.

[5] L.J. Soltzberg, A. Hagar, S. Kridaratikorn, A. Mattson, R. Newman, MALDI-TOF mass spectrometric identification, J. Am. Soc. Mass Spectrom. 18 (2007) 2001–2006, http://dx.doi.org/10.1016/j.jasms.2007.08.008.

[6] M.R. Williams, C. Moody, L.-A. Arceneaux, C. Rinke, K. White, M.E. Sigman, Analysis of black writing ink by electrospray ionization mass spectrometry, Forensic Sci. Int. 191 (2009) 97–103, http://dx.doi.org/10.1016/j.forsciint.2009.07.003.

[7] R.W. Jones, J.F. McClelland, Analysis of writing inks on paper using direct analysis in real time mass spectrometry, Forensic Sci. Int. 231 (2013) 73–81, http://dx.doi.org/10.1016/j.forsciint.2013.04.016.

[8] M. Ezcurra, J.M.G. Góngora, I. Maguregui, R. Alonso, Analytical methods for dating modern writing instrument inks on paper, Forensic Sci. Int. 197 (2010) 1–20, http://dx.doi.org/10.1016/j.forsciint.2009.11.013.

[9] C. Weyermann, D. Kirsch, C.C. Vera, B. Spengler, A GC/MS study of the drying of ballpoint pen ink on paper, Forensic Sci. Int. 168 (2007) 119–127, http://dx.doi.org/10.1016/j.forsciint.2006.06.076.

[10] G. Chiavari, S. Montalbani, S. Prati, Y. Keheyan, S. Baroni, Application of analytical pyrolysis for the characterisation of old inks, J. Anal. Appl. Pyrolysis 80 (2007) 400–405, http://dx.doi.org/10.1016/j.jaap.2007.04.011.

[11] Y.-Z. Liu, J. Yu, M.-X. Xie, Y. Chen, G.-Y. Jiang, Y. Gao, Studies on the degradation of blue gel pen dyes by ion-pairing high performance liquid chromatography and electrospray tandem mass spectrometry, J. Chromatogr. A 1125 (2006) 95–103, http://dx.doi.org/10.1016/j.chroma.2006.05.034.

[12] Y.-Z. Liu, J. Yu, M.-X. Xie, Y. Liu, J. Han, T.-T. Jing, Classification and dating of black gel pen ink by ion-pairing high-performance liquid chromatography, J. Chromatogr. A 1135 (2006) 57–64, http://dx.doi.org/10.1016/j.chroma.2006.09.031.

[13] C. Neumann, R. Ramotowski, T. Genessay, Forensic examination of ink by high-performance thin layer chromatography—the United States secret service digital ink library, J. Chromatogr. A 1218 (2011) 2793–2811, http://dx.doi.org/10.1016/j.chroma.2010.12.070.

[14] C. Vogt, J. Vogt, A. Becker, E. Rohde, Separation, comparison and identification of fountain pen inks by capillary electrophoresis with UV-visible and fluorescence detection and by proton-induced X-ray emission, J. Chromatogr. A 781 (1997) 391–405, http://dx.doi.org/10.1016/S0021-9673(97)00621-3.

[15] M. Gallidabino, C. Weyermann, R. Marquis, Differentiation of blue ballpoint pen inks by positive and negative mode LDI-MS, Forensic Sci. Int. 204 (2011) 169–178, http://dx.doi.org/10.1016/j.forsciint.2010.05.027.

[16] Y. Wu, C.X. Zhou, J. Yu, H.L. Liu, M.X. Xie, Differentiation and dating of gel pen ink entries on paper by laser desorption ionization- and quadruple-time of flight mass spectrometry, Dyes Pigments 94 (2012) 525–532, http://dx.doi.org/10.1016/j.dyepig.2012.03.005.

[17] L. Ng, L.K. Lafontaine, P. Brazeau, Ballpoint pen inks: characterization by positive and negative ion-electrospray ionization mass spectrometry for the forensic examination of writing inks, J. Forensic Sci. 47 (2002) 1238–1247.

[18] C. Weyermann, L. Bucher, P. Majcherczyk, W. Mazzella, C. Roux, P. Esseiva, Statistical discrimination of black gel pen inks analysed by laser desorption/ionization mass spectrometry, Forensic Sci. Int. 217 (2012) 127–133, http://dx.doi.org/10.1016/j.forsciint.2011.10.040.

[19] L. Heudt, D. Debois, T.A. Zimmerman, L. Köhler, F. Bano, F. Partouche, et al., Raman spectroscopy and laser desorption mass spectrometry for minimal destructive forensic analysis of black and color inkjet printed documents, Forensic Sci. Int. 219 (2012) 64–75, http://dx.doi.org/10.1016/j.forsciint.2011.12.001.

[20] D. S., J.E. Marrero, T. Cornell, K. Fowler, A. J., Analysis of pigmented inkjet printer inks and printed documents by laser desorption/mass spectrometry, J. Forensic Sci. 55 (2010) 129–135, http://dx.doi.org/10.1111/j.1556-4029.2009.01244.x.

[21] J.A. Denman, W.M. Skinner, K.P. Kirkbride, I.M. Kempson, Organic and inorganic discrimination of ballpoint pen inks by ToF-SIMS and multivariate statistics, Appl. Surf. Sci. 256 (2010) 2155–2163, http://dx.doi.org/10.1016/j.apsusc.2009.09.066.

[22] R.B. Cody, J.A. Laramee, H.D. Durst, Versatile new ion source for the analysis of materials in open air under ambient conditions, Anal. Chem. 77 (2005) 2297–2302, http://dx.doi.org/10.1021/ac050162j.

[23] J. Adams, Analysis of printing and writing papers by using direct analysis in real time mass spectrometry, Int. J. Mass Spectrom. 301 (2011) 109–126, http://dx.doi.org/10.1016/j.ijms.2010.07.025.

[24] S. Houlgrave, G.M. Laporte, J.C. Stephens, J.L. Wilson, The classification of inkjet inks using AccuTOF DART (direct analysis in real time) mass spectrometry-a preliminary study, J. Forensic Sci. 58 (2013) 813–821, http://dx.doi.org/10.1111/1556-4029.12048.

[25] R.G. Takats, Z. Wiseman, J.M. Cooks, Ambient mass spectrometry using desorption electrospray ionization (DESI): instrumentation, mechanisms and applications in forensics, chemistry, and biology, J. Mass Spectrom. 40 (2005) 1261–1275.

[26] L.S. Eberlin, R. Haddad, R.C. Sarabia Neto, R.G. Cosso, D.R.J. Maia, A.O. Maldaner, et al., Instantaneous chemical profiles of banknotes by ambient mass spectrometry, Analyst 135 (2010) 2533–2539, http://dx.doi.org/10.1039/c0an00243g.

[27] M.R.L. Paine, P.J. Barker, S.J. Blanksby, Characterising in situ activation and degradation of hindered amine light stabilisers using liquid extraction surface analysis-mass spectrometry, Anal. Chim. Acta 808 (2014) 190–198, http://dx.doi.org/10.1016/j.aca.2013.09.039.

[28] A. van Es, J. de Koeijer, G. van der Peijl, Discrimination of document paper by XRF, LA-ICP-MS and IRMS using multivariate statistical techniques, Sci. Justice 49 (2009) 120–126, http://dx.doi.org/10.1016/j.scijus.2009.03.006.

[29] K. Subedi, T. Trejos, J. Almirall, Forensic analysis of printing inks using tandem laser induced breakdown spectroscopy and laser ablation inductively coupled plasma mass spectrometry, Spectrochim. Acta, Part B 103–104 (2015) 76–83, http://dx.doi.org/10.1016/j.sab.2014.11.011.

[30] T. Trejos, A. Flores, J.R. Almirall, Micro-spectrochemical analysis of document paper and gel inks by laser ablation inductively coupled plasma mass spectrometry and laser induced breakdown spectroscopy, Spectrochim. Acta, Part B 65 (2010) 884–895, http://dx.doi.org/10.1016/j.sab.2010.08.004.

[31] T. Trejos, R. Corzo, K. Subedi, J. Almirall, Characterization of toners and inkjets by laser ablation spectrochemical methods and scanning electron microscopy-energy dispersive X-ray spectroscopy, Spectrochim. Acta, Part B 92 (2014) 9–22, http://dx.doi.org/10.1016/j.sab.2013.11.004.

[32] F.B. Gonzaga, W.F.D.C. Rocha, D.N. Correa, Discrimination between authentic and false tax stamps from liquor bottles using laser-induced breakdown spectroscopy and chemometrics, Spectrochim. Acta, Part B 109 (2015) 24–30, http://dx.doi.org/10.1016/j.sab.2015.04.011.

[33] M. Hoehse, A. Paul, I. Gornushkin, U. Panne, Multivariate classification of pigments and inks using combined Raman spectroscopy and LIBS, Anal. Bioanal. Chem. 402 (2012) 1443–1450, http://dx.doi.org/10.1007/s00216-011-5287-6.

[34] A. Kula, R. Wietecha-Posłuszny, K. Pasionek, M. Król, M. Woźniakiewicz, P. Kościelniak, Application of laser induced breakdown spectroscopy to examination of writing inks for forensic purposes, Sci. Justice 54 (2014) 118–125, http://dx.doi.org/10.1016/j.scijus.2013.09.008.

[35] D. Eikel, J. Henion, Liquid extraction surface analysis (LESA) of food surfaces employing chip-based nano-electrospray mass spectrometry, Rapid Commun. Mass Spectrom. 25 (2011) 2345–2354, http://dx.doi.org/10.1002/rcm.5107.

[36] N.L. Ledbetter, B.L. Walton, P. Davila, W.D. Hoffmann, R.N. Ernest, G.F.V. Iv, et al., Nanomanipulation-coupled nanospray mass spectrometry applied to the extraction and analysis of trace analytes found on fibers, J. Forensic Sci. 55 (2010) 1218–1221, http://dx.doi.org/10.1111/j.1556-4029.2010.01406.x.

[37] N. Wallace, E. Hueske, G.F. Verbeck, Science and justice ultra-trace analysis of illicit drugs from transfer of an electrostatic lift, Sci. Justice 51 (2011) 196–203, http://dx.doi.org/10.1016/j.scijus.2010.11.004.

[38] J.M. Brown, W.D. Hoffmann, C.M. Alvey, A.R. Wood, G.F. Verbeck, R.A. Petros, One-bead, one-compound peptide library sequencing via high-pressure ammonia cleavage coupled to nanomanipulation/nanoelectrospray ionization mass spectrometry, Anal. Biochem. 398 (2010) 7–14, http://dx.doi.org/10.1016/j.ab.2009.10.044.

[39] K. Clemons, J. Dake, E. Sisco, G.F. Verbeck, Trace analysis of energetic materials via direct analyte-probed nanoextraction coupled to direct analysis in real time mass spectrometry, Forensic Sci. Int. 231 (2013) 98–101, http://dx.doi.org/10.1016/j.forsciint.2013.04.022.

[40] P.J. Horn, U. Joshi, A.K. Behrendt, K.D. Chapman, G.F. Verbeck, On-stage liquid-phase lipid microextraction coupled to nanospray mass spectrometry for detailed, nanoscale lipid analysis, Rapid Commun. Mass Spectrom. 26 (2012) 957–962, http://dx.doi.org/10.1002/rcm.6194.

[41] V. Huynh, U. Joshi, J.M. Leveille, T.D. Golden, G.F. Verbeck, Nanomanipulation-coupled to nanospray mass spectrometry applied to document and ink analysis, Forensic Sci. Int. 242 (2014) 150–156, http://dx.doi.org/10.1016/j.forsciint.2014.06.037.

[42] V. Huynh, K.C. Williams, T.D. Golden, G.F. Verbeck, Investigation of falsified documents via direct analyte-probed nanoextraction coupled to nanospray mass spectrometry, fluorescence microscopy, and Raman spectroscopy, Analyst 140 (2015) 6553–6562, http://dx.doi.org/10.1039/c5an01026h.

[43] R. Stewart, L. Li, D. Thomas, Multipass laser ablation of three coloured ink from a paper substrate, J. Mater. Process. Technol. 114 (2001) 161–167, http://dx.doi.org/10.1016/S0924-0136(01)00728-2.

[44] R. Stewart, L. Li, D. Thomas, Laser Ablation of Multilayers of Ink From a Paper Substrate for Tactile Printing, 322000 301–305.

[45] X.Y. Ma, D. Shen, M. Luo, Y.W. Bo, J. Xu, C. Zhuo, Determination of blue ballpoint pen ink by laser ablation inductively coupled plasma mass spectrometry, Spectrosc. Spectr. Anal. 30 (2010) 2816–2819.

[46] R. Stewart, L. Li, D. Thomas, Multipass Laser Ablation of Three Coloured Ink From a Paper Substrate, 114, 2001.

[47] B.S. Kelly, J.S. Lindblom, Scientific Examination of Questioned Documents, CRC Press, Boca Raton, 2006.

[48] S. Thompson, T. Black, Forensic Human Identification, CRC Press, Boca Raton, 2006.

[49] J.L. Koenig, Spectroscopy of Polymers, Second Elsevier, New York, 1999.

[50] S. Han, C. Kim, D. Kwon, Thermal/oxidative degradation and stabilization of polyethylene glycol, Polymer 38 (1997) 317–323, http://dx.doi.org/10.1016/S0032-3861(97)88175-X.

[51] L. Boughen, J. Liggat, G. Ellis, Thermal degradation of polyethylene glycol 6000 and its effect on the assay of macroprolactin, Clin. Biochem. 43 (2010) 750–753, http://dx.doi.org/10.1016/j.clinbiochem.2010.02.012.

[52] J. Glastrup, Degradation of polyethylene glycol. A study of the reaction mechanism in a model molecule: tetraethylene glycol, Polym. Degrad. Stab. 52 (1996) 217–222, http://dx.doi.org/10.1016/0141-3910(95)00225-1.

[53] C. Weyermann, D. Kirsch, C. Costa-vera, B. Spengler, Photofading of ballpoint dyes studied on paper by LDI and MALDI MS, J. Am. Soc. Mass Spectrom. 17 (2006) 297–306, http://dx.doi.org/10.1016/j.jasms.2005.11.010.

[54] J.L. Campbell, M.N. Fiddler, K.E. Crawford, P.P. Gqamana, H.I. Kenttämaa, Analysis of polyethylene by using cyclopentadienyl cobalt chemical ionization combined with laser-induced acoustic desorption/fourier transform ion cyclotron resonance mass spectrometry, Anal. Chem. 77 (2005) 4020–4026, http://dx.doi.org/10.1021/ac048409k.

[55] A. Anne, M.A. Bahri, A. Chovin, C. Demaille, C. Taofifenua, Probing the conformation and 2D-distribution of pyrene-terminated redox-labeled poly(ethylene glycol) chains end-adsorbed on HOPG using cyclic voltammetry and atomic force

electrochemical microscopy, Phys. Chem. Chem. Phys. 16 (2014) 4642–4652, http://dx.doi.org/10.1039/C3CP54720E.
[56] J. Ding, H. Gu, S. Yang, M. Li, J. Li, H. Chen, Selective detection of diethylene glycol in toothpaste products using neutral desorption reactive extractive electrospray ionization tandem mass spectrometry, Anal. Chem. 81 (2009) 8632–8638, http://dx.doi.org/10.1021/ac9013594.
[57] J.N. Hemenway, T.C. Carvalho, V.M. Rao, Y. Wu, J.K. Levons, A.S. Narang, S.R. Paruchuri, H.J. Stamato, V. S.A., Formation of reactive impurities in aqueous and neat polyethylene glycol 400 effects of antioxidants and oxidation inducers, J. Pharm. Sci. 101 (2010) 3305–3318, http://dx.doi.org/10.1002/jps.
[58] J.S. Becker, M.V. Zoriy, C. Pickhardt, N. Palomero-Gallagher, K. Zilles, Imaging of copper, zinc, and other elements in thin section of human brain samples (hippocampus) by laser ablation inductively coupled plasma mass spectrometry, Anal. Chem. 77 (2005) 3208–3216, http://dx.doi.org/10.1021/ac040184q.
[59] J. Feldmann, A. Kindness, P. Ek, Laser ablation of soft tissue using a cryogenically cooled ablation cell, J. Anal. At. Spectrom. 17 (2002) 813–818, http://dx.doi.org/10.1039/b201960d.
[60] M.B. Fricker, D. Kutscher, B. Aeschlimann, J. Frommer, R. Dietiker, J. Bettmer, et al., High spatial resolution trace element analysis by LA-ICP-MS using a novel ablation cell for multiple or large samples, Int. J. Mass Spectrom. 307 (2011) 39–45, http://dx.doi.org/10.1016/j.ijms.2011.01.008.
[61] I. Konz, B. Fernández, M.L. Fernández, R. Pereiro, A. Sanz-Medel, Design and evaluation of a new Peltier-cooled laser ablation cell with on-sample temperature control, Anal. Chim. Acta 809 (2014) 88–96, http://dx.doi.org/10.1016/j.aca.2013.11.040.
[62] B.P. Davies, S.J. Hertig, C.A. Gilbride, Security Supervision and Management, Fourth Butterworth-Heinemann:Elsevier, Waltham, 2015.